Thermally Assisted Recording Pushes Magnetic Storage Densities beyond Traditional Limits

The desire to increase magnetic storage densities requires downscaling of the bit dimensions, which are currently limited to ~50 nm. In the past, this was made possible by reducing the grain size of the recording media. However, the decrease in grain size will eventually reach the superparamagnetic limit, at which thermal energy is sufficient to randomize the magnetization direction. Consequently, further increases in recording densities require materials with higher magnetic anisotropy energy. While these materials are available, they cannot be used because the magnetic field of the recording heads is insufficient to write these materials. Recently, a group of researchers at the IBM T.J. Watson Research Center in Yorktown Heights, N.Y., demonstrated that by thermally assisting the recording process, very high-density magnetization patterns could be written, therefore breaking the record on magnetic storage density.

In an article published in *Applied Physics Letters* on February 2, researchers H.F. Hamann, Y.C. Martin, and H.K. Wickramasinghe described their experiment in detail. They placed an atomic force microscope tip (radius, ~5 nm) in close vicinity to a magnetic film of TbFe on a mica substrate or a Co/Pt multilayer film, also on a mica substrate. The tip was heated by a laser diode. Some of the energy was transferred on a very local scale from the tip to the magnetic film, which was then heated to close to its Curie temperature. The magnetic bias field was applied to align the magnetization in the heated region. The heated region of the film had a substantially lower coercivity and could be magnetized with a small field.

On the basis of magnetic force microscopy measurements, the researchers said that the recorded spot sizes are less than 30 nm in diameter. The magnetization patterns obtained on the thin film correspond to a storage density of ~400 Gbit/in^2. The researchers believe this is the highest magnetic storage density reported. Furthermore, by thermal modeling, they predicted that an even smaller heated spot size can be realized. That means, potentially, a recording density of >1 Tbit/in.^{2} can be achieved.

SHIMING WU

Photodetectors Fabricated Using Electrostatic Self-Assembly

Organic semiconducting polymers are attractive materials for use in photovoltaic (PV) detectors because of their tunability and flexibility. However, excitons in organic PV devices are easily quenched and have limited diffusion lengths, making it essential to have good control over layer thicknesses. Using spin coating, it is often difficult to obtain the desired ultrathin polymer films. Electrostatic self-assembly can produce very thin films through alternate deposition of oppositely charged polyelectrolytes. As reported in the February 10 issue of *Chemistry of Materials*,

Femtosecond Lasers Facilitate Writing of 3D Colored Images with Precipitation of Au Nanoparticles in Glass

A number of researchers have previously reported the application of femtosecond (fs) laser pulses to three-dimensional (3D) direct writing of structures buried in materials. In the February 15 issue of *Optics Letters*, J. Qiu of the Chinese Academy of Sciences and the Japan Science and Technology Agency, K. Hirao of Kyoto University, and colleagues with the Photon Craft Project describe a femtosecond laser-assisted method that precipitates nanoparticles within a silicate glass with 3D control of the area that is precipitated. This enables the creation of well-defined structures within a monolith of glass. The researchers' interest in developing this approach was piqued because the optical properties of noble-metal nanoparticles differ from those of their bulk form due to the quantum size effect and increased surface area, resulting in much larger third-order nonlinearities and an ultrafast nonlinear response time.

The silicate glass had a composition of $70SiO_2 \cdot 10CaO \cdot 20Na_2O$ (mol%) and was doped with 0.1 mol% Au_20_3. An 800 nm laser system with 120 fs pulses at 1 kHz was used to structurally modify the glass. The high intensity of the beam, due to the tightly focused spot (9 μm spot diameter at the beam waist in the glass) and short pulse duration, causes multiphoton ionization of the glass. During the ionization, an electron–hole plasma is formed that recombines to produce white-light emission. However, some of the free electrons from the ionized glass are captured by the Au ions to form Au atoms. The process also forms hole-trapped nonbridging oxygen sites due to the ionization of the glass. After the glass is annealed for 30 min at 550°C, the Au atoms precipitate into nanoparticles. Transmission electron microscopy analysis confirmed the existence of the Au nanoparticles in the irradiated area, with sizes ranging from 5 nm to 10 nm. Spectroscopic analysis showed an increase in the absorption in the irradiated sample at wavelengths of 310 nm, 420 nm, and 620 nm, all of which can be ascribed to hole–trap centers at the nonbridging oxygen atoms. An absorption peak at 530 nm was observed after annealing. The peak wavelength increased with increased annealing time, which points to the surface plasmon resonance of the particles as the source of this absorption line.

By changing the position and depth of focus of the beam, the location of the nanoparticles can be controlled, thus allowing for the writing of 3D images, as shown in the Figure with the image of a butterfly. For the intensity used to construct the butterfly, illumination with the 9 μm spot resulted in a region ~40 μm in diameter in which the properties of the glass were changed. The researchers determined that the size of the region affected could be controlled from a few hundred nanometers to a few millimeters by altering the intensity and the spot size of the incident laser beam. The researchers also used an optical Kerr shutter experiment to measure the temporal response of the nanoparticles, obtaining a Kerr signal response of 240 fs for a 500 fs pulse width (inside the glass). This development has applications in industrial art, high-density memory storage, and all-optical ultrafast switching for optical communications.

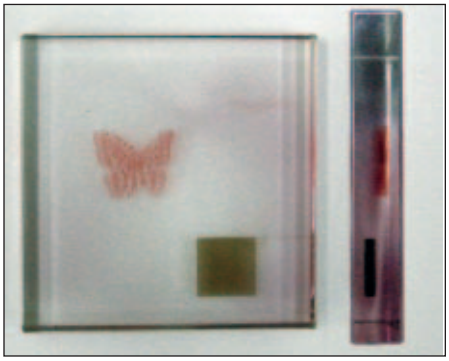

Figure. A butterfly created within a glass sample by femtosecond laser pulse excitation followed by oven annealing. The gray image has not been annealed. The size of the glass sample is 50 mm × 50 mm × 8 mm. The width of the butterfly is ~15 mm. Front and side views are presented.

https://doi.org/10.1557/mrs2004.43 Published online by Cambridge University Press

a multidisciplinary group from the University of Hong Kong has used this method to fabricate efficient PV devices.

W.K. Chan and co-workers used poly(*p*-phenylene vinylene) (PPV) functionalized with ruthenium terpyridine complexes as the photosensitizer for these devices. Sulfonated polyaniline (SPAN) served as the hole-transport material. Each device was fabricated by sequentially dipping an indium tin oxide glass slide into solutions of SPAN and ruthenium-functionalized PPV. After depositing a defined number of SPAN-PPV bilayers, the researchers coated the thin film with a 40 nm aluminum electrode layer.

Thin films made up of 13, 20, and 30 bilayers were fabricated and found to have overall thicknesses of 110 nm, 150 nm, and 190 nm, respectively. The researchers controlled the device thickness by varying the dipping conditions. They measured current–voltage characteristics for all three devices, in the dark and under optical illumination. The maximum short-circuit current and open-circuit voltage were both exhibited by the device comprising 13 bilayers. The team said that although this device has lower absorbance than those with more bilayers, its performance may be due to a lower serial resistance. The external quantum efficiency of the devices was measured and found to agree well with the absorption spectrum of the device. For the device with 13 bilayers, the maximum efficiency was 2.2%, while the device with 30 bilayers showed an efficiency of 5%. This maximum efficiency occurs at an optical wavelength of ~510 nm, in agreement with the maximum absorption of the ruthenium dye. The researchers conclude that the enhancement of the efficiency is due to the presence of the metal sensitizers.

The researchers propose that by working with a mixture of metal complexes with varying absorbance maxima, it may be possible to use electrostatic self-assembly to prepare detectors with photosensitivity over a wide range.

CATHERINE OERTEL

Simulations Show Formation of Inorganic Nanotubes within SWNTs

Low-dimensional inorganic crystalline structures analogous to single-walled carbon nanotubes (SWNTs), called ionic inorganic nanotubes (IINTs), have been prepared with both physical and chemical methods. The structure of IINTs formed by filling SWNTs with molten salts can be related to crystalline sheets, just as SWNTs are related to graphene sheets. Computer models have been employed to determine the stabilities of IINTs but heretofore have not been used to identify new IINT structures worthy of experimental investigation. Recently, however, M. Wilson at the Department of Chemistry, University College London, used atomistic computer models to simulate the formation of a range of novel IINTs by filling SWNTs with bulk inorganic liquids.

In an article published in the February issue of *Nano Letters*, Wilson, a Royal Society Research Fellow, described the controlled formation of IINTs within SWNTs using a relatively simple atomistic computer model. Effective pair potentials control the short-range ion–ion and ion–carbon interactions. With polarization effects also accounted for and parameters chosen to reflect a tetrahedral ion coordination environment, a typical bulk crystal ground state results. The SWNTs, formed by folding single graphene sheets, were treated as fixed atomistic tubes. Molecular dynamics simulation techniques were applied to fill the SWNTs with bulk molten ions and to form the IINTs. Molecular mechanics geometry optimizations were then used to produce an effective IINT formation phase diagram, which shows that the dominant factor controlling IINT morphology is the SWNT diameter. For example, both (5,2) and (4,3) IINTs, whose diameters are 7.29 Å and 7.10 Å, respectively, form within (19,0) or (11,11) SWNTs, whose diameters are 14.90 Å and

https://doi.org/10.1557/mrs2004.43 Published online by Cambridge University Press